Journal of Molecular Liquids 336 (2021) 116266

Contents lists available at ScienceDirect

Journal of Molecular Liquids

journal homepage: www.elsevier.com/locate/molliq

Hybrid combinations of graphene nanoplatelets and phosphonium ionic liquids as lubricant additives for a polyalphaolefin

Khodor I. Nasser, José M. Liñeira del Río, Enriqueta R. López *, Josefa Fernández

Laboratory of Thermophysical and Tribological Properties, Nafomat Group, Department of Applied Physics, Faculty of Physics, University of Santiago de Compostela, 15782 Santiago de Compostela, Spain

ARTICLE INFO

Article history:
Received 11 January 2021
Revised 10 April 2021
Accepted 19 April 2021
Available online 24 April 2021

Keywords:
Ionic liquids
Graphene derivatives
Hybrid additives
Friction
Wear
Viscosity

ABSTRACT

Tribological performance of three ionic liquids (ILs), trihexyltetradecylphosphonium bis(2-ethylhexyl) phosphate (IL1), tributylethylphosphonium diethylphosphate (IL2) and trihexyltetradecylphosphonium bis(2,4,4-trimethylpentyl)phosphinate (IL3) combined with graphene nanoplatelets (GnP) as hybrid additives for a polyalphaolefin (PAO 32) base oil was studied. For this purpose, several dispersions were prepared by mixing, stirring, and then sonicating according to the following combinations: PAO 32 + (*a* wt%) IL + (*b* wt%) GnP, where *a* and *b* represent the concentration of the additives added to the PAO 32 base oil. In this study *a* is 0 or 1 and *b* is 0.05 or 0.1. Three PAO 32 + 1 wt% IL mixtures were also prepared. Thermophysical properties and stability against sedimentation of the dispersions were studied by means of a rotational viscometer and visual observation, respectively. Furthermore, friction and wear behaviors were analyzed using a ball-on-disk configuration tribometer operating in rotational mode and both a 3D optical profiler and a scanning electronic microscope, respectively. Confocal Raman microscopy was used to identify compounds in the tribofilms formed on the wear tracks. The hybrid combinations of PAO 32/ILs/GnP improved the friction reduction of the corresponding binary PAO 32/GnP nanolubricants and PAO 32/IL mixtures. Interestingly, the hybrid dispersions with low concentrations of GnP (with 0.05 wt% GnP) are more effective than those of 0.1 wt% GnP. Results also show that the addition of both 0.05 wt% graphene nanoplatelets and 1 wt% IL led to friction reductions up to 36% and wear reductions up to 27%, compared with the capabilities of neat PAO 32. IL1 and IL3, containing the trihexyltetradecylphosphonium cation, generate the hybrid lubricants with the best combined properties (stability, viscosity and tribological properties) of all the lubricants tested.

1. Introduction

Tribological properties such as friction and wear are directly related to energy consumption in several industrial sectors (transportation, energy generation, manufacturing, . . .) [1]. These properties are considered important in classical and innovative machinery due to their influence in enhancing energy efficiency and life span. A good lubrication helps to minimize friction and wear between two surfaces in contact.

Due to their special properties, several nanomaterials are considered excellent additives to enhance lubricant performance [2–5]. Graphene, the first 2D crystal ever isolated, is a single graphite layer with exceptional properties. Nevertheless, mass-production methods to obtain defect-free monolayer graphene have not been developed yet. Contrastingly, graphene nanoplatelets, GnP, short stacks of graphene sheets in a platelet shape, are commercially available and less expensive [6]. Several authors [7–12] found that GnPs have excellent properties as lubricant additives. Different mechanisms were identified to explain how nanoadditives enhance the tribological performance of neat lubricants. These mechanisms can be classified into two main groups [4]. The first one involves the direct effect of nanoadditives including the ball bearings effect or protective tribo-film formation. Ball bearing is discarded in the case of GnP additives due their non-spherical shape. The second group is related to surface improvements by mending (by nanoparticle deposition in the valleys of the contact surfaces) or polishing effects. Different studies concerning 2D additives [5,13] revealed that these materials can easily enter between friction surfaces due to their ultra-thin layer structure and extremely low shear strength between the layers, consequently preventing the direct contact of the rubbing surfaces and decreasing friction. The main lubrication mechanisms related to 2D materials are both film formation and mending effects [14]. Through tribo-

* Corresponding author.
E-mail address: enriqueta.lopez@usc.es (E.R. López).

https://doi.org/10.1016/j.molliq.2021.116266
0167-7322/

logical measurements of graphene platelets dispersed in a mineral oil, Lin et al. [7] concluded that these additives form protective deposited films to prevent the rubbing surfaces from coming into direct contact and improve the tribological behavior of the oil. Nevertheless, agglomeration problems limit the varied applications of 2D materials in the field of lubrication [15].

Moreover, ionic liquids (ILs), which were used as neat lubricants [16], are also proposed as oils additives [17]. Phosphonium ILs are considered potential lubricant additives because of their interesting properties (good miscibility in oils, and their antiwear and anticorrosion performances) being their organic phosphorus relevant in tribo-chemistry [17–25]. In addition, phosphonium salts do not react with most organic compounds, and are compatible with most commonly used lubricant additives and are reliable as such [26]. When used as lubricant additives, ILs tend to form protective tribofilms on the rubbing contact areas [17]. It was pointed out that the protective tribofilm formation is through the tribochemical reaction of ILs and/or their decomposition products with the contact surfaces and/or wear debris at the lubricating interfaces [17]. Furthermore, due to the positive charge induced on rubbing surfaces by tribo-stress, anions interact strongly with oppositely charged surfaces [27]. As a result, when surfaces lubricated with an IL are compressed, lubricating films will remain in place at higher forces than with a comparable molecular lubricant [27].

Polyalphaolefins (PAOs) are saturated hydrocarbons synthesized by polymerization of alphaolefins followed by hydrogenation, which are classified as group IV base oils according to API classification [28–30]. PAOs are used for automotive engines, in formulating hydraulic fluids, compressor oils and high temperature gear and bearing industrial lubricants [30–32]. There are several studies on the tribological performance of either nanoparticles, NPs, or ILs as additives in PAO 4 [33–35], PAO 6 [36–43], PAO 8 [44,45] PAO 10 [46–48], PAO 32 [49], and PAO 40 [42,50].

The hybrid combinations of ILs and nanomaterials as additives in lubricant oils may lead to interesting positive synergies. In this regard, adding ILs to nanolubricants may improve both the stability and the tribological behavior [11,49,51–54]. Nevertheless, studies on the combined effects of ILs and NPs as oil additives are uncommon. Sanes *et al.* [53] evaluated a 5 wt% dispersion of 0.1 wt% graphene in an IL as friction-reducing and antiwear hybrid additive of an additive-free isoparaffinic base oil. These authors concluded that there are synergistic effects between both additives, concluding that the IL presence would prevent oxidation while the graphene may increase the load-carrying ability of the lubricant.

Regarding polyalphaolefins oils, there are only two articles that studied the synergies of NPs and ILs. In the first one, Seymour *et al.* [51] studied the possible antifriction synergies between hairy silica NPs (HNP) and an oil-miscible phosphonium-phosphate ionic liquid (IL) dispersed in PAO 4. These authors obtained a friction decrease with the hybrid combinations of up to 23% compared with 2% HNP alone in PAO and of up to 35% compared to the PAO mixed with 2% IL. Furthermore, Nasser et al. [49] studied the tribological synergies of hybrid nanostructure combinations of three phosphonium ionic liquids and hexagonal boron nitride (h-BN) as additives of PAO 32 base oil. It was observed that the hybrid additives improve, in general, the tribological performance of the lubricant rather than being used separately, being the maximum reductions at 353.15 K of 28% and 65% in friction and wear, respectively, in comparison to the neat oil. Hence, the combinations of ILs and nanomaterials forming hybrid structures as additives of PAOs are hardly known, and the synergistic effects are not yet clear due to limited investigations in this field.

Aiming to contribute to a better knowledge of these combinations, in this work the tribological performance, thermophysical properties and dispersion stability of several combinations of both NPs and ILs as hybrid additive of PAO 32 are studied. Thus, graphene nanoplatelets (GnP) and trihexyltetradecylphosphonium bis(2-ethylhexyl)phosphate (IL1), tributylethylphosphonium diethylphosphate (IL2) or trihexyltetradecylphosphonium bis(2,4,4-trimethylpentyl)phosphinate (IL3) were chosen as hybrid additives of a polyalphaolefin (PAO 32). The effect of the structure of ILs and concentration of GnP in all the properties were analyzed. PAO 32 was chosen since it is the base oil of the current lubricant formulations in wind turbine gearboxes.

2. Experimental section

2.1. Materials

Table 1 presents the base oil, the nanoadditive and the ILs investigated in this study. PAO 32 was supplied by Repsol. Both Fourier transform infrared (FTIR) and Raman spectra of aliquots of this oil were reported previously [49]. Graphene nanoplatelets having CAS number 1034343-98-0, 99.5% purity, average particle diameter of 15 μm and 11 to 15 nm thickness were supplied by Iolitec. Liñeira del Río *et al.* [8] and Guimarey *et al.* [55] characterized two samples of these nanoplatelets by means of energy-dispersive X-ray, Raman spectroscopies as well as transmission and scanning electron microscopies, showing bent and wrinkled shapes.

The ionic liquids trihexyltetradecylphosphonium bis(2-ethylhexyl)phosphate (IL1), tributylethylphosphonium diethylphosphate (IL2) and trihexyltetradecylphosphonium bis(2,4,4-trimethylpentyl)phosphinate (IL3) were supplied by Iolitec. In a previous work [49], FTIR and Raman spectra of these ILs were reported.

2.2. Sample preparation

Using a two-step method, two binary dispersions were prepared: PAO 32 + 0.05 wt% GnP, PAO 32 + 0.1 wt% GnP. In addition, the following hybrid dispersions: PAO 32 + 1 wt% IL1 + 0.05 wt% GnP, PAO 32 + 1 wt% IL2 + 0.05 wt% GnP, PAO 32 + 1 wt% IL3 + 0.05 wt% GnP, PAO 32 + 1 wt% IL1 + 0.1 wt% GnP, PAO 32 + 1 wt% IL2 + 0.1 wt% GnP and PAO 32 + 1 wt% IL3 + 0.1 wt% GnP, were prepared using Sanes *et al.* [53] method. Thus, IL1, IL2 or IL3 samples were separately mixed with GnP nanopowders in an agate mortar and continuously stirred for 10 min. Each GnP/IL sample was mixed with PAO 32 base oil to obtain the hybrid dis-

Table 1
Main information of materials used in this work.

Chemical name	Reduced name	Supplier	CAS number	Purity*
Polyalphaolefin 32	PAO 32	Repsol	533903–84-3	
Graphene nanoplatelets	GnP	Iolitec	1034343–98-0	0.95
Trihexyltetradecylphosphonium bis(2-ethylhexyl)phosphate (IL1)	$[P_{6,6,6,14}][DEHP]$	Iolitec	1092655–30-5	>0.98
Tributylethylphosphonium diethylphosphate (IL2)	$[P_{2,4,4,4}][DEP]$	Iolitec	20445–94-7	>0.95
Trihexyltetradecylphosphonium bis(2,4,4-trimethylpentyl)phosphinate (IL3)	$[P_{6,6,6,14}][(iC_8)_2PO_2]$	Iolitec	465527–58-6	>0.9

* Provided by the supplier.

persions. PAO 32 + 1 wt% IL1, PAO 32 + 1 wt% IL2 and PAO 32 + 1 wt % IL3 mixtures were also prepared. A Sartorius MC 210P high accurate balance (precision of 0.00001 g) was used to determine the mass concentrations of PAO 32, GnP and ILs. Finally, the mixtures and dispersions were continuously sonicated for four hours in a Fisherbrand TM 11203 ultrasonic bath at effective power of 180 W and frequency of 37 kHz. Two replicates of mixtures and dispersions were made, one for visual stability analysis and the other for tribological study.

2.3. Thermophysical characterization

Density and viscosity at atmospheric pressure over a temperature ranging from 278.15 K to 373.15 K of PAO 32/GnP and PAO 32/IL/GnP dispersions were measured by means of a SVM 3000 rotational Stabinger viscometer from Anton Paar [56]. The viscosity index was also experimentally determined according to ASTM D2270 using this device. Expanded uncertainties (k = 2) are 0.0005 $g{\cdot}cm^{-3}$ for density, 0.02 K for temperatures from 288.15 to 378.15 K and 0.05 K outside this range, and 1% for dynamic viscosity. Details of the device and procedure were reported previously [57,58].

2.4. Tribological tests

Friction tests for PAO 32 neat lubricant, the three mixtures (PAO 32/IL), the two nanolubricants (PAO 32/GnP) and the six hybrid nanolubricants (PAO 32/ILs/GnP) were performed using a CSM Standard tribometer with a ball-on-disk configuration. During tests, a fixed AISI 52100/535A99 chrome steel ball (6 mm diameter and hardness 58–66 Rockwell Scale) contacts with an AISI 52100/535A99 chrome steel disk (surface finish Ra < 0.02 μm, hardness 190–210 Hv30 and diameter 10 mm) which rotates with a linear speed of 0.10 m s^{-1} (3 mm radius) for 3400 s, at room temperature, ~294 K and under a normal load of 20 N. Hexane and hot air were used to clean and dry the specimens before these tests. 0.15 mL of the lubricant were placed on the disk surface. Three replicates of each test were performed and the mean values reported as the friction coefficients. After friction tests, the disks were cleaned in an ultrasonic bath containing hexane for one minute and then dried with hot air. Wear on disks was analyzed with a 3D optical profiler (Sensofar S neox) through width, cross section area, depth, and roughness measurements of the worn surfaces. The cross-sectional area was determined using the section profile by subtracting the sum of areas of the profiles for the material displaced on both sides of the worn track from the worn area. A Carl Zeiss FESEM ULTRA Plus Scanning Electron Microscope (SEM) was also used to analyze the worn surface, as well as a WITec alpha300R + confocal Raman microscope to obtain composition information at the wear scar.

3. Results and discussion

3.1. Stability of the mixtures and nanodispersions

The eight dispersions were kept at room temperature and observed weekly after the preparation. For both PAO 32 + GnP dispersions no signs of sedimentation appear for 240 days after preparation, as shown in Figs. 1 and 2. In contrast, for both nanodispersions containing IL2, stability worsening was observed. In fact, for PAO 32 + 1 wt% IL2 + 0.1 wt% GnP sample, sedimentation was visualized 60 days after preparation, whereas for PAO

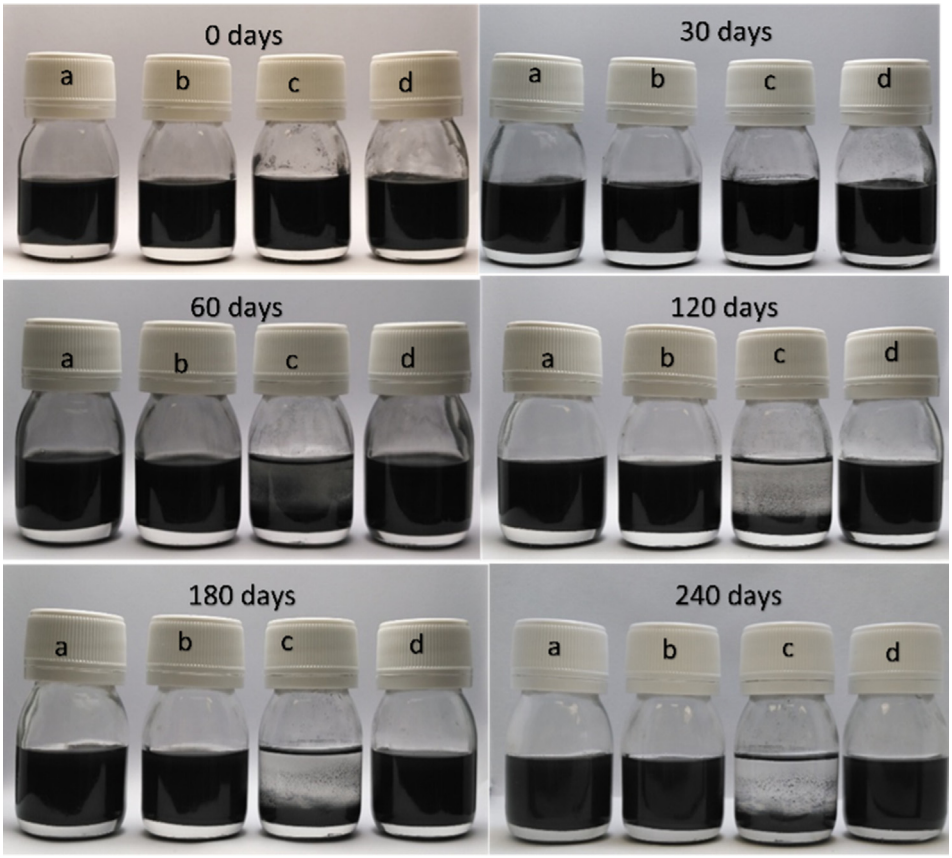

Fig. 1. Samples photos: (a) PAO 32 + 0.1 wt% GnP, (b) PAO 32 + 1 wt% IL1 + 0.1 wt% GnP, (c) PAO 32 + 1 wt% IL2 + 0.1 wt% GnP, (d) PAO 32 + 1 wt% IL3 + 0.1 wt% GnP.

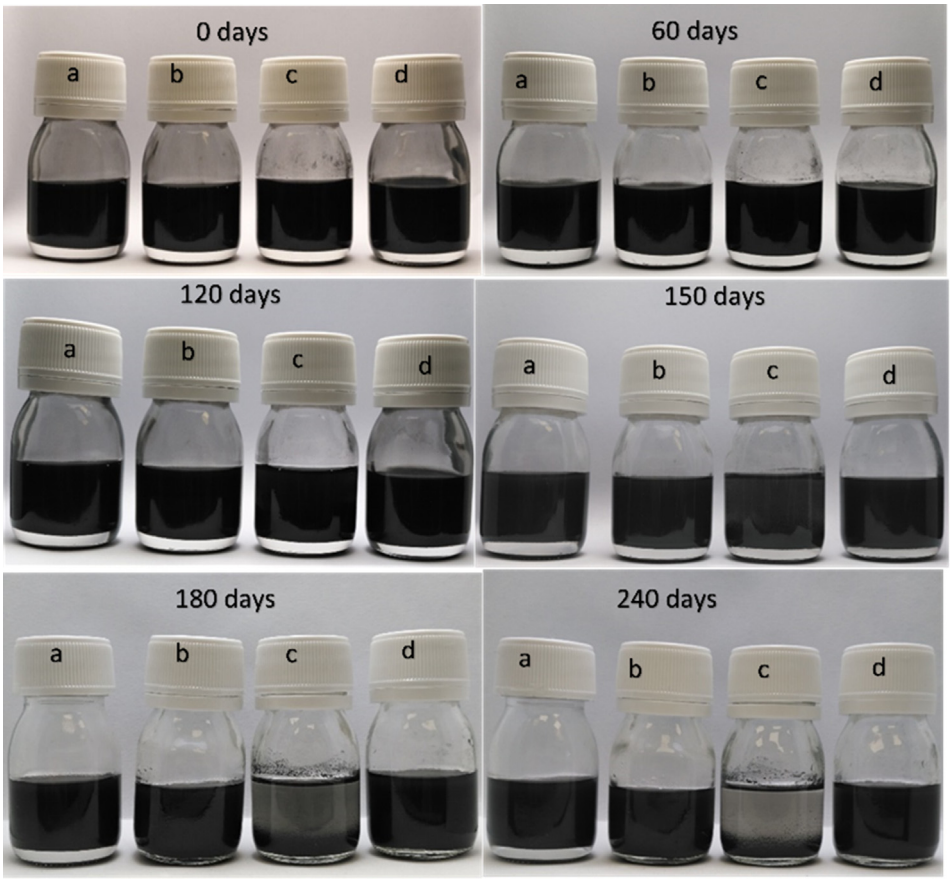

Fig. 2. Samples photos: (a) PAO 32 + 0.05 wt% GnP (b) PAO 32 + 1 wt% IL1 + 0.05 wt% GnP, (c) PAO 32 + 1 wt% IL2 + 0.05 wt% GnP, (d) PAO 32 + 1 wt% IL3 + 0.05 wt% GnP.

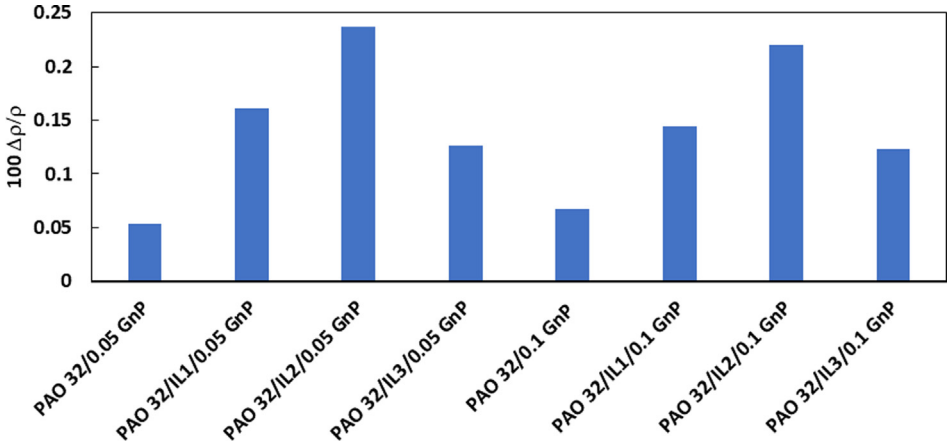

Fig. 3. Percentage average absolute density increase, 100 Δρ/ρ, of the nanodispersions containing PAO 32 respect to density of PAO 32 in the temperature range from 278.15 K to 373.15 K.

32 + 1 wt% IL2 + 0.05 wt% GnP sample, it occurred after 150 days. Regarding IL1 and IL3 nanodispersions, no signs of sedimentation appeared for 240 days after preparation. As in previous work [49] in which h-BN is used instead GnP, the poorest time stability also corresponded to the hybrid nanodispersions containing IL2, but the h-BN/IL2 dispersion stability is not worse than that of the h-BN nanodispersion. Thus, concerning stability, negative synergies were found between IL2 and GnP as hybrid additives in PAO 32.

3.2. Thermophysical characterization

Dynamic viscosity (η) and density (ρ) values at several temperatures together with viscosity index (VI) of the eight dispersions are reported in Tables S1-S3, η and ρ experimental data were reported previously [49] for PAO 32 as well as for PAO 32 + 1 wt % IL1, PAO 32 + 1 wt% IL2 and PAO 32 + 1 wt% IL3 mixtures. The average increase in density values of dispersions in comparison to PAO 32 due to GnP and to both GnP and ILs addition ranged

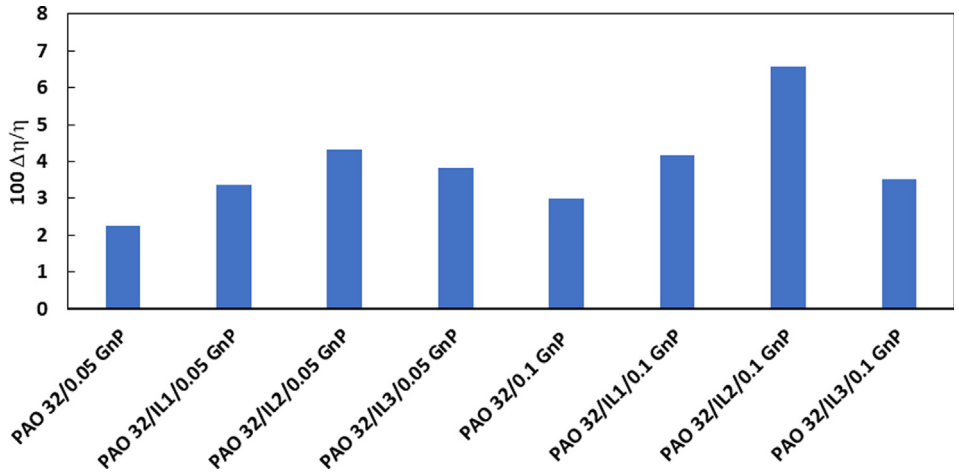

Fig. 4. Percentage average absolute dynamic viscosity increase, 100 $\Delta\eta/\eta$, of the nanodispersions containing PAO 32 respect to the in the temperature range from 278.15 K to 373.15 K.

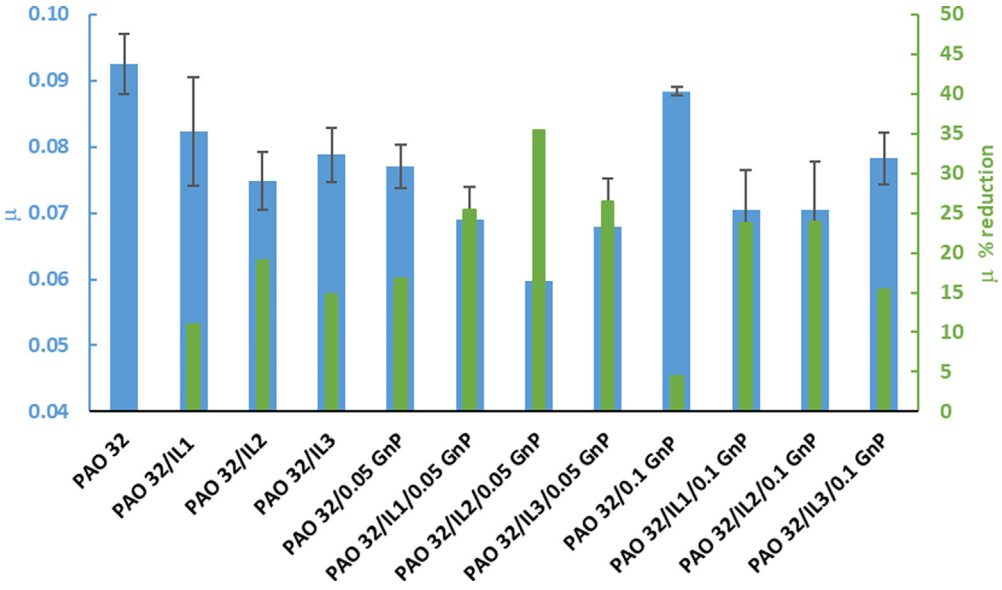

Fig. 5. Average friction coefficient (μ) and its corresponding reduction using different lubricants compared to PAO 32 base oil at room temperature.

Table 2
Average values of the friction coefficient (μ), wear scar width (WSW), cross-section area, and maximum depth of the wear track together with their standard deviations (σ) and % reductions compared with PAO 32 for all lubricants at room temperature.

Lubricant	μ	σ	% friction reduction	WSW/ μm	σ	% width reduction	Area / μm^2	σ	% Area reduction	Max depth/ μ m	σ	% depth reduction
PAO 32	0.0932	0.0046	–	260	3	–	160	3	–	1.301	0.014	–
PAO 32 + 1 wt% IL1	0.0823	0.0082	11	249	1	4.2	150	2	6.3	1.183	0.013	9.2
PAO 32 + 1 wt% IL2	0.0749	0.0043	19	248	2	4.6	142	3	11	1.112	0.012	15
PAO 32 + 1 wt% IL3	0.0788	0.0041	15	250	2	3.8	155	3	3.1	1.223	0.010	6.0
PAO 32 + 0.05 wt% GnP	0.0770	0.0033	17	243	1	6.5	140	3	12	1.110	0.009	15
PAO 32 + 1 wt% IL1 + 0.05 wt% GnP	0.0690	0.0049	25	229	2	12	126	2	21	0.993	0.005	24
PAO 32 + 1 wt% IL2 + 0.05 wt% GnP	0.0591	0.0031	36	226	3	13	124	3	23	0.951	0.018	27
PAO 32 + 1 wt% IL3 + 0.05 wt% GnP	0.0684	0.0071	27	230	3	12	128	3	20	1.010	0.012	23
PAO 32 + 0.1 wt% GnP	0.0884	0.0007	5.2	245	1	5.8	150	2	6.3	1.190	0.014	8.5
PAO 32 + 1 wt% IL1 + 0.1 wt% GnP	0.0714	0.0061	23	240	1	7.7	136	3	15	1.053	0.013	18
PAO 32 + 1 wt% IL2 + 0.1 wt% GnP	0.0704	0.0073	24	235	3	9.6	130	3	19	1.000	0.018	23
PAO 32 + 1 wt% IL3 + 0.1 wt% GnP	0.0783	0.0039	15	241	3	7.3	131	3	18	1.100	0.018	15

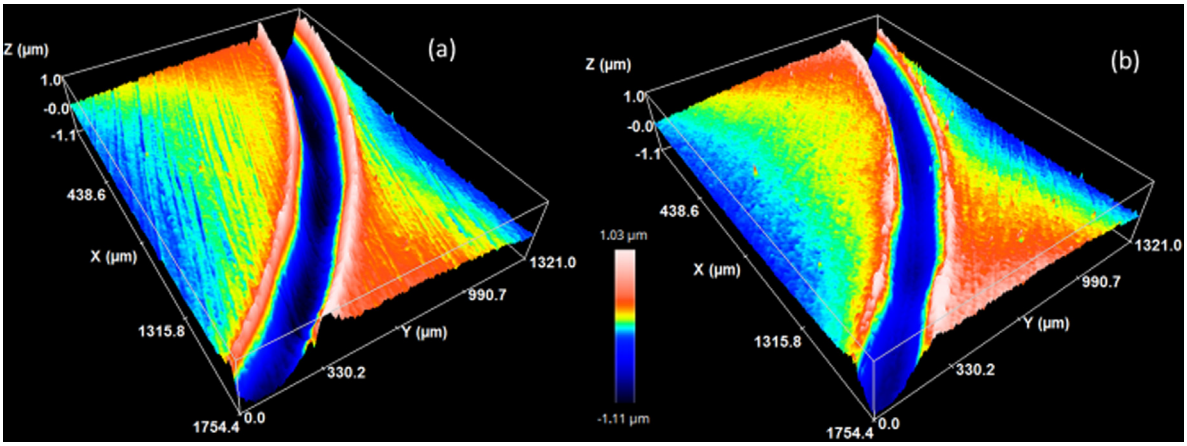

Fig. 6. 3D-Optical micrographs (10x) of the wear track at the disk surface lubricated by PAO 32 (a) and PAO 32 + 1 wt% IL2 + 0.05 wt% GnP (b) at room temperature.

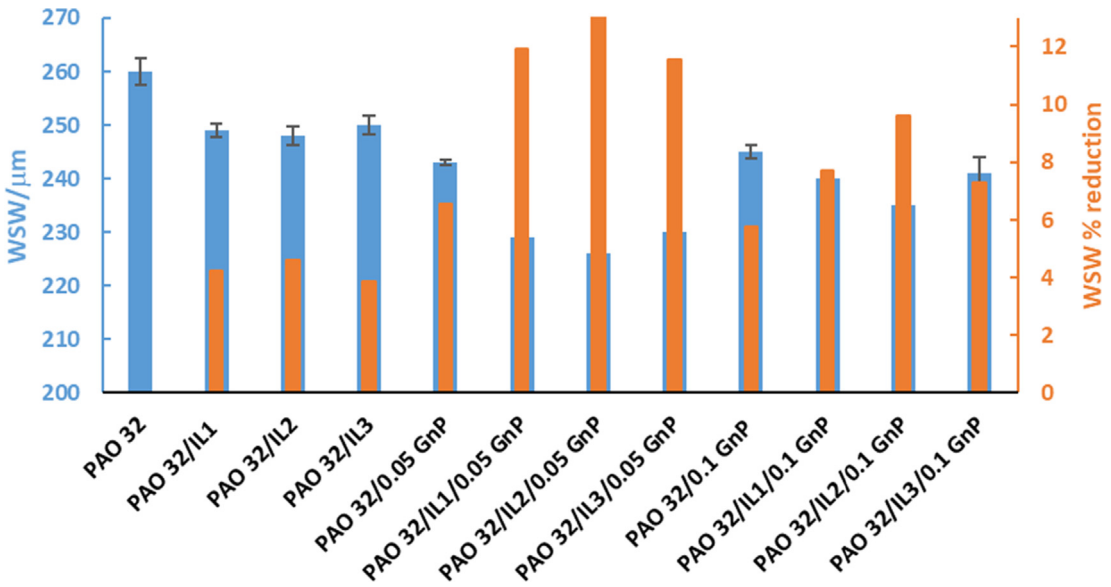

Fig. 7. Wear scar width (μm) at the surface of the disks using different lubricants, and the corresponding reduction (%) compared with PAO 32 base oil performance at room temperature.

between 0.05 and 0.24%, i.e., one to four times the density uncertainty. The average absolute rise in density over the whole temperature range is plotted in Fig. 3, where it can be seen that the largest contribution to this increase is due to the hybrid additive GnP/IL2, the IL with the shortest anion and cation alkyl chains ([$P_{2,4,4,4}$][DEP]).

Fig. 4 shows the average absolute rise in viscosity over the whole temperature range. For all dispersions, the viscosity values were slightly greater than those of PAO 32 values. The average increase due to GnP and to both GnP and ILs addition, ranged between 2.2% and 6.6% (the uncertainty of the viscosity values is 1%). The highest average relative dynamic viscosity increment corresponds to PAO 32/IL2/0.1%wt GnP nanodispersion. Table S3 reports the viscosity index, VI, of PAO 32, the mixtures and nanodispersions. VI changes were small, ranging from −1.7% to 0.53%.

3.3. Friction behavior and lubrication regime

The average friction coefficient values (μ) of the three trials measured for each lubricant at room temperature are plotted in Fig. 5 and reported in Table 2. All additives enhanced the antifriction behavior of PAO 32, specifically friction coefficient values range from 0.059 to 0.088 corresponding to reductions of 36 to 5%, respectively. 0.1 wt% GnP individual addition resulted in the lowest efficient nanolubricant with 5% reduction, whereas the most effective antifriction nanolubricant was PAO 32 + 1 wt% IL2 + 0.05 wt% GnP (36% reduction). The hybrid combinations of PAO 32/ILs/GnP improved the friction reduction of the corresponding binary PAO 32/GnP nanolubricants. Interestingly, the hybrid dispersions with low concentrations of GnP (with 0.05 wt% GnP) are more effective than those of 0.1 wt% GnP. Optimal graphene derivative concentrations in oils have been found in recent years [8,59–62].

3.4. Surface analysis and wear behavior

3D optical images of disk wear scar tested with PAO 32 and PAO 32 + 1 wt% IL2 + 0.05 wt% GnP at room temperature obtained with the 3D optical profiler are shown in Fig. 6. As can be observed, the wear scar on the plate is slightly wavy, indicating that plastic flow occurs [8]. Table 2 displays the averages of wear scar width (WSW), cross-section area, and of the maximum depth of the wear track (WTD) calculated from the disk surface analysis. All the average values were obtained from three repetitions. Fig. 7 shows the

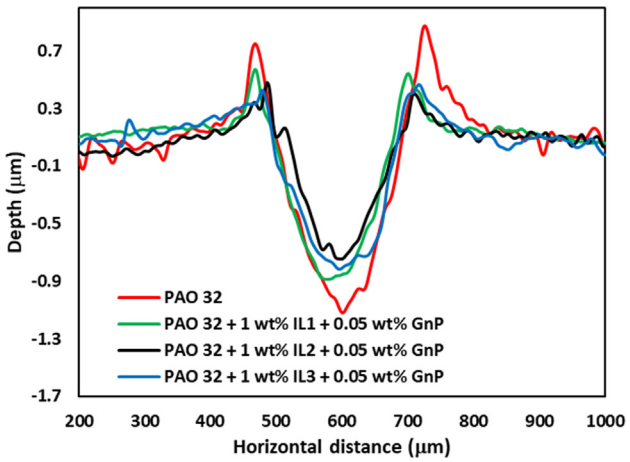

Fig. 8. Wear track cross section profile at the lubricated disk surfaces for PAO 32 and PAO 32/1 wt% IL/0.05 wt% GnP.

average WSW values and the reductions for all the mixtures and nanodispersions with respect to the WSW corresponding to the wear scar lubricated with PAO 32 without additives. This base oil showed the maximum WSW, 260 μm, followed by lower values for all the lubricants containing one type of additive with 243, 245, 248, 249 and 250 μm corresponding to PAO 32 + 0.05 wt% GnP, PAO 32 + 0.1 wt% GnP, PAO 32 + 1 wt% IL2, PAO 32 + 1 wt% IL1, and PAO 32 + 1 wt% IL3, respectively.

The hybrid combination of ILs and GnP resulted in additional reductions of WSW, cross section area, and maximum depth. This performance was enhanced when low concentrations of GnP were added to the lubricant. Thus, in terms of WSW, the addition of 0.05 wt% GnP instead of 0.1 wt% GnP slightly improved anti-wear capabilities from 7.7%, 9.6% and 7.3% to 12%, 13% and 12% for nanodispersions containing IL1, IL2 and IL3, respectively. Fig. 8 shows the 2D profiles of the grooves inside the lubricated disks for PAO 32 and the hybrid nanolubricants PAO 32/1 wt% IL/0.05 wt% GnP, with the lower scar corresponding to PAO 32/IL2/GnP.

SEM images of the worn disks lubricated with PAO 32, the mixtures and hybrid nanodispersions are shown in Figs. S1-S3. In all the cases smooth surfaces without signs of plowing or abrasion were obtained, although plastic deformation is observed in agreement with the 3D profiles (Fig. 6). This fact agrees with previous results obtained by Pamies et al. [63], who studied the antiwear performance of ionic liquid + graphene dispersions finding that graphene prevents the formation of large abrasive particles.

The 3D Optical Profiler, under 4287 ISO standard and Gaussian filter of long wavelength cut-off equals 0.25 mm, was also used to measure the average roughness (*Ra*) value of the wear scar surface of the lubricated disks. *Ra* measured values are plotted in Fig. 9. As shown, the worn surfaces lubricated with the three mixtures and the eight nanolubricants displayed lower roughness than that of PAO 32. The most significant *Ra* reductions were achieved by using 1 wt% ILs/ 0.05 wt% GnP as hybrid additives into the base oil. *Ra* was reduced in comparison to PAO 32 37, 36 and 35% for IL2, IL1 and IL3, respectively. Hence for smoothing the contact surfaces, 1 wt% ILs/0.05 wt% GnP as hybrid additives present better positive synergies than 1 wt% ILs/0.1 wt% GnP (Fig. 9).

Raman spectra and elemental mapping of the compounds found on the worn surfaces lubricated with the base oil, the mixtures and the nanodispersions were performed at a wavelength of 532 nm. PAO 32 and the three ILs have very similar spectrum shapes [49]. Therefore, to analyze exactly which material is presented at the worn surface, the most dissimilar peaks were identified to distinguish between PAO 32 and the ILs. All mappings (Figs. 11 and S4-S13) showed areas where the spectrum coincides with that of PAO 32 (blue areas), areas where the spectrum corresponds to carbon (in red) which would be due to carbonization of the base oil at sliding surfaces, resulted from local high temperature [64] or during Raman spectrum tests, as well as areas corresponding to iron oxides (in green). Generally, oxides were observed for all the worn surfaces.

Neat PAO 32. Raman spectra reveals formation of boundary tribofilms composed of iron oxides, carbon, and the oil itself. This result is compatible with that obtained by Ratoi *et al.* [65] who performed tribological tests in a ball-on-disk setup test rig, using a similar tribo-pair. These authors concluded that, among other effects, a tribofilm is built through oxide formation and lubricant degradation on the wear track leading to smoother wear. Through X-ray photoelectron spectroscopy they observed that those tribofilms are mainly formed by carbon, iron, and oxygen. Khodor

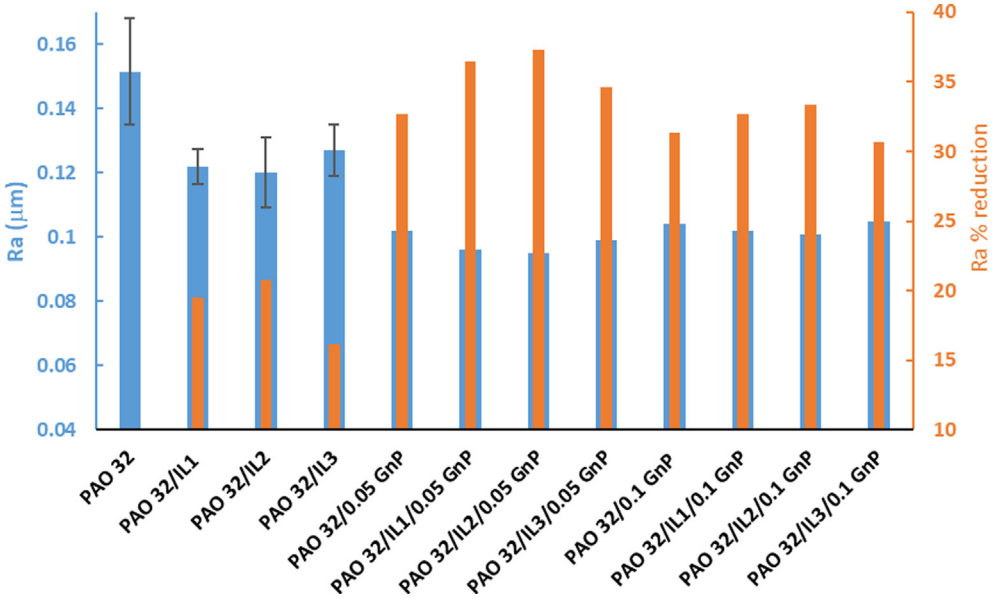

Fig. 9. Average Roughness values (*Ra*) at the contact surface of the disks lubricated by the different lubricants at room temperature.

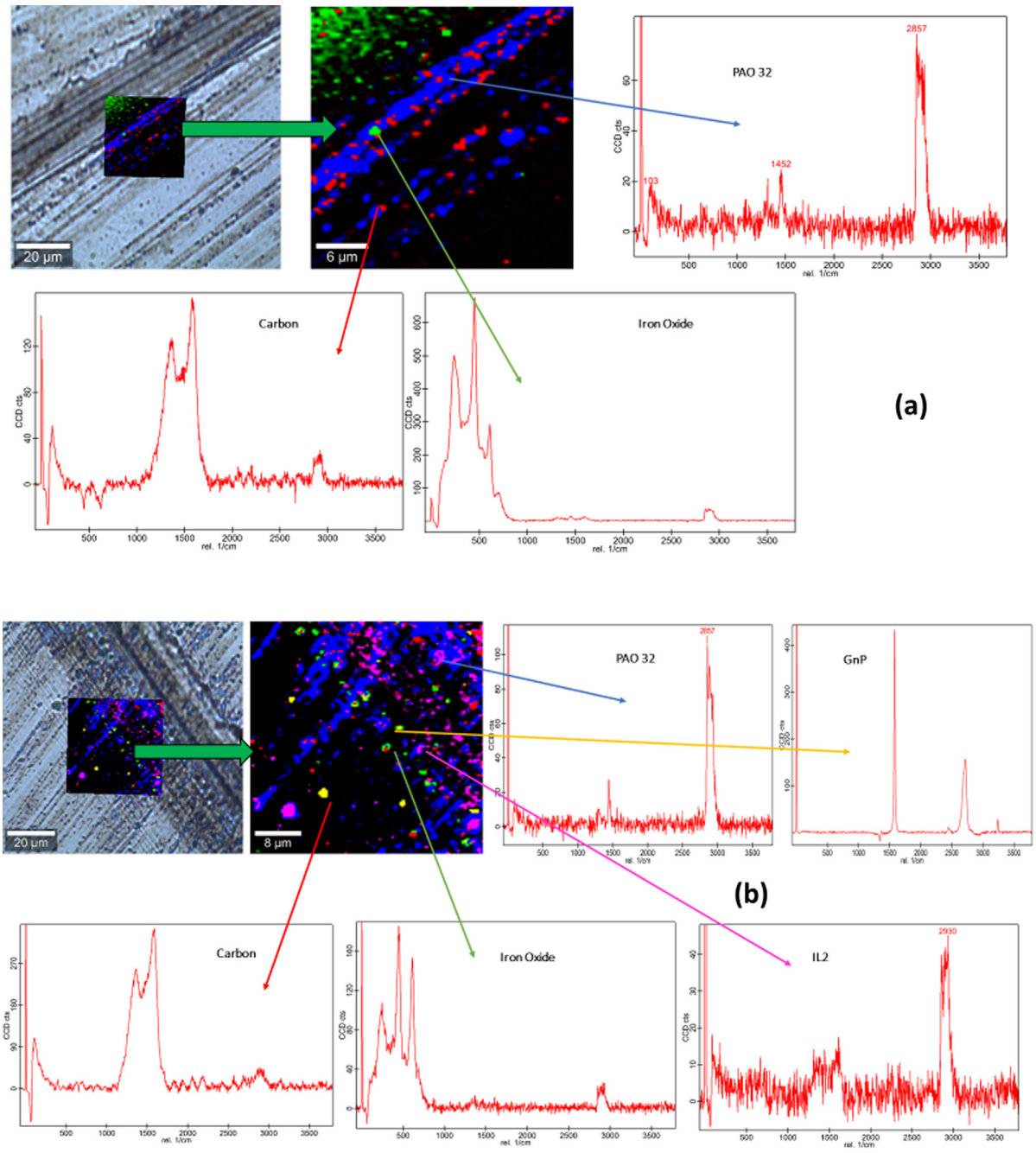

Fig. 10. Raman spectra and element map combination at the worn surface lubricated by: (a) PAO 32 and (b) PAO 32 + 1 wt% IL2 + 0.05 wt% GnP at room temperature.

et al. [49] also found, using Raman mappings for a worn surface tested with PAO 32, areas with iron oxides and carbon for different specimens tested at 353.15 K.

PAO 32/IL mixtures. The three PAO 32/IL mixtures improve the tribological performance of neat PAO 32. The best antifriction and antiwear capabilities correspond to the mixture with IL2, [$P_{2,4,4,4}$][DEP]. From the three ILs evaluated, IL2 has the shortest alkyl chains in both anion and cation, being linear for both ions. As regards to Raman results (Figs. S4-S6), IL protective tribofilms (pink areas) were observed and likely formed through the tribochemical reaction with rubbing surfaces. No stronger differences on these area sizes were observed either in the worn surface lubricated with mixtures containing IL2 and IL3, being smaller for IL1. Furthermore, IL addition to PAO 32 reduces the presence of iron oxides (green areas of the mappings) on the worn surface. The following trend was observed for the size of these areas IL3 < IL2 < IL1. Hence, the most significant mechanisms of the tribological behavior of PAO 32/IL mixtures is the tribofilm formation due to the IL and the iron oxides. Similar behavior was obtained by Nasser et al. [49], who performed similar tests at 353.15 K, finding iron oxide areas slightly higher for IL2 and IL3 mixtures and slightly lower for IL1.

PAO 32/GnP nanodispersions. GnP nanoadditives improve the tribological performance of PAO 32. This enhancement is nonetheless higher in the case of the dispersion with the lower GnP content. Thus, the optimum composition in GnP is 0.05 wt%. However, the size of the GnP areas (yellow, Figs. S7 and S8) of the Raman mappings of worn surfaces tested with PAO 32/0.1 wt% GnP are higher than the corresponding areas for the disk lubricated with PAO 32/0.05 wt% GnP. The mechanisms of the tribological enhance-

ments of GnP are the tribofilm and mending effects, which reduce the roughness of the worn surface around 30% (Fig. 9) in comparison to that tested with neat PAO 32.

IL/GnP synergies as hybrid additives. As aforementioned, PAO 32/IL/GnP hybrid dispersions enhance the tribological performances of both, the corresponding mixtures, and the corresponding binary dispersions. A similar behavior was obtained by Liñeira del Río et al. [11]. These authors found positive synergies between IL2 and GnP or h-BN nanoparticles. As regards Raman mappings (Fig. 10b and S9-S13), the presence of hybrid additives reduces the oxide area sizes (green), especially for PAO 32 + 1 wt% IL1 + 0.05 wt% GnP and PAO 32 + 1 wt% IL2 + 0.05 wt% GnP. For nanoadditive distribution (yellow areas) on the worn surfaces lubricated by PAO 32/IL/GnP, the higher the GnP content, the greater the area. Regarding IL tribofilms (pink) no strong differences in area sizes were observed, being slightly higher for PAO 32 + 1 wt% IL2 + 0.05 wt% GnP.

Boundary tribofilms composed of ILs, iron oxides, carbon and the oil itself evidenced by Raman microscopy, prevent the direct contact of the mating surfaces, acting as outstanding stress reducers by producing smoother wear tracks during friction tests, due to the presence of GnP which act as an efficient stress releaser when load is applied and easily slides due to weak interlayer bonds without fracture [66], but also due to phosphonium ILs which react with the surface to form protective tribofilms [67–69].

4. Conclusions

The hybrid combination of different concentrations of GnP nanoparticles and three phosphonium based ILs as additives to PAO 32 base oil for a steel-steel contact at room temperature and mixed conditions was investigated. Stability, and both thermophysical and tribological properties were analyzed. The Raman analyses performed on the worn surfaces of the plates reveal the presence of protective tribofilms that contain GnP and ILs.

The final goal of these fundamental studies is to provide the industry with knowledge about reliable additives that can be used in real applications. With this goal in mind, PAO 32/IL2/0.05 wt% GnP dispersion is not the best option since it worsens the stability of the corresponding PAO 32/GnP dispersions. Moreover, IL2 is the additive that led to the most viscosity rises. Furthermore, IL2 has another weakness: it is corrosive in humid environments [49]. Results show that the addition of both 0.05 wt% graphene nanoplatelets and 1 wt% of any of the ILs (IL1 or IL3) containing the cation $[P_{6,6,6,14}]^+$ gives rise to the hybrid lubricants with the best combined capabilities. Consequently, and considering that the tribological performance of hybrid dispersions PAO 32/IL/0.05 wt% GnP containing IL1 and IL3 (both with the cation $[P_{6,6,6,14}]^+$) also improve the tribological behavior of PAO 32, either one could work as potential anti-friction and anti-wear additives for PAO 32.

CRediT authorship contribution statement

Khodor I. Nasser: Validation, Formal analysis, Writing - original draft, Visualization. **José M. Liñeira del Río:** Formal analysis, Writing - review & editing. **Enriqueta R. López:** Methodology, Formal analysis, Writing - review & editing. **Josefa Fernández:** Conceptualization, Writing - review & editing, Supervision, Project administration.

Declaration of Competing Interest

The authors declare that they have no known competing financial interests or personal relationships that could have appeared to influence the work reported in this paper.

Acknowledgments

Authors acknowledge Repsol for providing us the PAO 32 sample. Authors are grateful for the use of the RIAIDT-USC analytical facilities, and would like to especially thank Mr. Ezequiel Vázquez for his useful advice. This work was supported by the Spanish Ministry of Science, Innovation and Universities and the ERDF programme (FEDER in Spanish) through ENE2017-86425-C2-2-R project, and by the Xunta de Galicia (ED431D 2017/06, ED431E 2018/08 and ED431C 2020/10). These funders also financed the acquisition of the 3D Optical Profile (UNST15-DE-3156).

Appendix A. Supplementary material

Supplementary data to this article can be found online at https://doi.org/10.1016/j.molliq.2021.116266.

References

[1] K. Holmberg, A. Erdemir, Influence of tribology on global energy consumption, costs and emissions, Friction 5 (2017) 263–284, https://doi.org/10.1007/s40544-017-0183-5.
[2] Y. Chen, P. Renner, H. Liang, Dispersion of nanoparticles in lubricating oil: a critical review, Lubricants 7 (2019) 7, https://doi.org/10.3390/lubricants7010007.
[3] S. Shahnazar, S. Bagheri, S.B. Abd Hamid, Enhancing lubricant properties by nanoparticle additives, Int. J. Hydrogen Energy 41 (2016) 3153–3170, https://doi.org/10.1016/j.ijhydene.2015.12.040.
[4] M. Gulzar, H.H. Masjuki, M.A. Kalam, M. Varman, N.W.M. Zulkifli, R.A. Mufti, R. Zahid, Tribological performance of nanoparticles as lubricating oil additives, J. Nanopart. Res. 18 (2016) 223, https://doi.org/10.1007/s11051-016-3537-4.
[5] W. Dai, B. Kheireddin, H. Gao, H. Liang, Roles of nanoparticles in oil lubrication, Tribol. Int. 102 (2016) 88–98, https://doi.org/10.1016/j.triboint.2016.05.020.
[6] P. Cataldi, A. Athanassiou, I.S. Bayer, Graphene nanoplatelets-based advanced materials and recent progress in sustainable applications, Applied Sciences 8 (2018) 1438, https://doi.org/10.3390/app8091438.
[7] J. Lin, L. Wang, G. Chen, Modification of graphene platelets and their tribological properties as a lubricant additive, Tribol. Lett. 41 (2011) 209–215, https://doi.org/10.1007/s11249-010-9702-5.
[8] J.M. Liñeira del Río, M.J.G. Guimarey, M.J.P. Comuñas, E.R. López, A. Amigo, J. Fernández, Thermophysical and tribological properties of dispersions based on graphene and a trimethylolpropane trioleate oil, J. Mol. Liq. 268 (2018) 854–866, https://doi.org/10.1016/j.molliq.2018.07.107.
[9] S.S.N. Azman, N.W.M. Zulkifli, H. Masjuki, M. Gulzar, R. Zahid, Study of tribological properties of lubricating oil blend added with graphene nanoplatelets, J. Mater. Res. 31 (2016) 1932–1938, https://doi.org/10.1557/jmr.2016.24.
[10] W. Rashmi, M. Khalid, Y.L. Xiao, T.C.S.M. Gupta, G.Z. Arwin, Tribological studies on graphene/TMP based nanolubricant, J. Eng. Sci. Technol. 12 (2017) 365–373. https://pureapps2.hw.ac.uk/ws/portalfiles/portal/16440665/12_2_6.pdf.
[11] J.M. Liñeira del Río, E.R. López, J. Fernández, Synergy between boron nitride or graphene nanoplatelets and tri(butyl)ethylphosphonium diethylphosphate ionic liquid as lubricant additives of triisotridecyltrimellitate oil, J. Mol. Liq. 301 (2020), https://doi.org/10.1016/j.molliq.2020.112442 112442.
[12] B. Suresha, G. Hemanth, Ananthapadmanabha, G. Kulkarni, Role of graphene nanoplatelets on tribological behaviour of madhuca indica oil, AIP Conference Proceedings 2247 (2020) 040008. https://doi.org/10.1063/5.0004145.
[13] L. Liu, M. Zhou, X. Li, L. Jin, G. Su, Y. Mo, L. Li, H. Zhu, Y. Tian, Research progress in application of 2D materials in liquid-phase lubrication system, Materials (Basel) 11 (2018) 1314, https://doi.org/10.3390/ma11081314.
[14] G. Paul, H. Hirani, T. Kuila, N.C. Murmu, Nanolubricants dispersed with graphene and its derivatives: an assessment and review of the tribological performance, Nanoscale 11 (2019) 3458–3483, https://doi.org/10.1039/C8NR08240E.
[15] L. Liu, M. Zhou, L. Jin, L. Li, Y. Mo, G. Su, X. Li, H. Zhu, Y. Tian, Recent advances in friction and lubrication of graphene and other 2D materials: Mechanisms and applications, Friction 7 (2019) 199–216, https://doi.org/10.1007/s40544-019-0268-4.
[16] A.E. Somers, P.C. Howlett, D.R. MacFarlane, M. Forsyth, A review of ionic liquid lubricants, Lubricants 1 (2013) 3–21, https://doi.org/10.3390/lubricants1010003.
[17] Y. Zhou, J. Qu, Ionic liquids as lubricant additives: a review, ACS Appl. Mater. Interfaces 9 (2017) 3209–3222, https://doi.org/10.1021/acsami.6b12489.
[18] X. Liu, F. Zhou, Y. Liang, W. Liu, Tribological performance of phosphonium based ionic liquids for an aluminum-on-steel system and opinions on lubrication mechanism, Wear 261 (2006) 1174–1179, https://doi.org/10.1016/j.wear.2006.03.018.
[19] I. Otero, E.R. López, M. Reichelt, M. Villanueva, J. Salgado, J. Fernández, Ionic liquids based on phosphonium cations as neat lubricants or lubricant additives

for a steel/steel contact, ACS Appl. Mater. Interfaces 6 (2014) 13115–13128, https://doi.org/10.1021/am502980m.
[20] M.A. Gutierrez, M. Haselkorn, P. Iglesias, The lubrication ability of ionic liquids as additives for wind turbine gearboxes oils, Lubricants 4 (2016) 14, https://doi.org/10.3390/lubricants4020014.
[21] S. Cowie, P.K. Cooper, R. Atkin, H. Li, Nanotribology of ionic liquids as lubricant additives for alumina surfaces, J. Phys. Chem. C 121 (2017) 28348–28353, https://doi.org/10.1021/acs.jpcc.7b09879.
[22] P.K. Cooper, J. Staddon, S. Zhang, Z.M. Aman, R. Atkin, H. Li, Nano- and macroscale study of the lubrication of titania using pure and diluted ionic liquids, Front. Chem. 7 (2019), https://doi.org/10.3389/fchem.2019.00287.
[23] R. González, J.L. Viesca, A.H. Battez, M. Hadfield, A. Fernández-González, M. Bartolomé, Two phosphonium cation-based ionic liquids as lubricant additive to a polyalphaolefin base oil, J. Mol. Liq. 293 (2019), https://doi.org/10.1016/j.molliq.2019.111536 111536.
[24] A. Hernández Battez, C.M.C.G. Fernandes, R.C. Martins, M. Bartolomé, R. González, J.H.O. Seabra, Two phosphonium cation-based ionic liquids used as lubricant additive: Part I: Film thickness and friction characteristics, Tribol. Int. 107 (2017) 233–239, https://doi.org/10.1016/j.triboint.2016.10.048.
[25] R. González, M. Bartolomé, D. Blanco, J.L. Viesca, A. Fernández-González, A.H. Battez, Effectiveness of phosphonium cation-based ionic liquids as lubricant additive, Tribol. Int. 98 (2016) 82–93, https://doi.org/10.1016/j.triboint.2016.02.016.
[26] L. Weng, X. Liu, Y. Liang, Q. Xue, Effect of tetraalkylphosphonium based ionic liquids as lubricants on the tribological performance of a steel-on-steel system, Tribol. Lett. 26 (2007) 11–17, https://doi.org/10.1007/s11249-006-9175-8.
[27] H. Li, M.W. Rutland, R. Atkin, Ionic liquid lubrication: influence of ion structure, surface potential and sliding velocity, PCCP 15 (2013) 14616–14623, https://doi.org/10.1039/c3cp52638k.
[28] S. Jiang, S. Li, L. Liu, L. Wang, N. Mominou, The tribological properties and tribochemical analysis of blends of poly alpha-olefins with neopentyl polyol esters, Tribol. Int. 86 (2015) 42–51, https://doi.org/10.1016/j.triboint.2015.01.015.
[29] W.R. Murphy, D.A. Blain, A.S. Galiano-Roth, P.A. Galvin, Benefits of synthetic lubricants in industrial applications, J. Synth. Lubr. 18 (2002) 301–325, https://doi.org/10.1002/jsl.3000180406.
[30] L.R. Rudnick, Polyalphaolefins, in: L.R. Rudnick (Ed.), Synthetic, Mineral Oils, and Bio-based Lubricants: Chemistry and Technology, CRC Press, Taylor and Francis Group, Boca Raton, FL, 2013, pp. 3–40.
[31] J.B. Gajewski, M.J. Głogowski, Anti-wear additive content in fully synthetic PAO and PAG base oils and its effect on electrostatic and tribological phenomena in a rotating shaft–oil–lip seal system, J. Phys. Conf. Ser. 418 (2013), https://doi.org/10.1088/1742-6596/418/1/012045 012045.
[32] J.B. Gajewski, M.J. Głogowski, Influence of additives blended with motor base oils on the braking torque under an auxiliary external DC electric field, J. Electrostat. 71 (2013) 1100–1103, https://doi.org/10.1016/j.elstat.2013.10.011.
[33] J. Qu, D.G. Bansal, B. Yu, J.Y. Howe, H. Luo, S. Dai, H. Li, P.J. Blau, B.G. Bunting, G. Mordukhovich, D.J. Smolenski, Antiwear performance and mechanism of an oil-miscible ionic liquid as a lubricant additive, ACS Appl. Mater. Interfaces 4 (2012) 997–1002, https://doi.org/10.1021/am201646k.
[34] Y. Zhou, J. Dyck, T.W. Graham, H. Luo, D.N. Leonard, J. Qu, Ionic liquids composed of phosphonium cations and organophosphate, carboxylate, and sulfonate anions as lubricant antiwear additives, Langmuir 30 (2014) 13301–13311, https://doi.org/10.1021/la5032366.
[35] J. Qu, H. Luo, M. Chi, C. Ma, P.J. Blau, S. Dai, M.B. Viola, Comparison of an oil-miscible ionic liquid and ZDDP as a lubricant anti-wear additive, Tribol. Int. 71 (2014) 88–97, https://doi.org/10.1016/j.triboint.2013.11.010.
[36] Y. Zhang, S. Zhang, D. Sun, G. Yang, C. Gao, C. Zhou, C. Zhang, P. Zhang, Wide adaptability of Cu nano-additives to the hardness and composition of DLC coatings in DLC /PAO solid-liquid composite lubricating system, Tribol. Int. 138 (2019) 184–195, https://doi.org/10.1016/j.triboint.2019.05.043.
[37] A. Hernández Battez, R. González, J.L. Viesca, J.E. Fernández, J.M. Díaz Fernández, A. Machado, R. Chou, J. Riba, CuO, ZrO_2 and ZnO nanoparticles as antiwear additive in oil lubricants, Wear 265 (2008) 422–428. https://doi.org/10.1016/j.wear.2007.11.013.
[38] P.U. Aldana, F. Dassenoy, B. Vacher, T. Le Mogne, B. Thiebaut, WS_2 nanoparticles anti-wear and friction reducing properties on rough surfaces in the presence of ZDDP additive, Tribol. Int. 102 (2016) 213–221, https://doi.org/10.1016/j.triboint.2016.05.042.
[39] D. Blanco, R. González, A. Hernández Battez, J.L. Viesca, A. Fernández-González, Use of ethyl-dimethyl-2-methoxyethylammonium tris(pentafluoroethyl) trifluorophosphate as base oil additive in the lubrication of TiN PVD coating, Tribol. Int. 44 (2011) 645–650, https://doi.org/10.1016/j.triboint.2011.01.004.
[40] D. Blanco, A.H. Battez, J.L. Viesca, R. González, A. Fernández-González, Lubrication of CrN coating with ethyl-dimethyl-2-methoxyethylammonium tris(pentafluoroethyl)trifluorophosphate ionic liquid as additive to PAO 6, Tribol. Lett. 41 (2011) 295–302, https://doi.org/10.1007/s11249-010-9714-1.
[41] T. Espinosa, J. Sanes, A.-E. Jiménez, M.-D. Bermúdez, Protic ammonium carboxylate ionic liquid lubricants of OFHC copper, Wear 303 (2013) 495–509, https://doi.org/10.1016/j.wear.2013.03.041.
[42] R. Rosentsveig, A. Gorodnev, N. Feuerstein, H. Friedman, A. Zak, N. Fleischer, J. Tannous, F. Dassenoy, R. Tenne, Fullerene-like MoS_2 nanoparticles and their tribological behavior, Tribol. Lett. 36 (2009) 175–182, https://doi.org/10.1007/s11249-009-9472-0.
[43] V.B. Niste, H. Tanaka, M. Ratoi, J. Sugimura, WS_2 nanoadditized lubricant for applications affected by hydrogen embrittlement, RSC Adv. 5 (2015) 40678–40687, https://doi.org/10.1039/c5ra03127c.
[44] L. Peña-Parás, J. Taha-Tijerina, L. Garza, D. Maldonado-Cortés, R. Michalczewski, C. Lapray, Effect of CuO and Al_2O_3 nanoparticle additives on the tribological behavior of fully formulated oils, Wear 332–333 (2015) 1256–1261, https://doi.org/10.1016/j.wear.2015.02.038.
[45] S. Paskvale, M. Remškar, M. Čekada, Tribological performance of TiN, TiAlN and CrN hard coatings lubricated by MoS_2 nanotubes in polyalphaolefin oil, Wear 352–353 (2016) 72–78, https://doi.org/10.1016/j.wear.2016.01.020.
[46] N.G. Demas, E.V. Timofeeva, J.L. Routbort, G.R. Fenske, Tribological effects of BN and MoS_2 nanoparticles added to polyalphaolefin oil in piston skirt/cylinder liner tests, Tribol. Lett. 47 (2012) 91–102, https://doi.org/10.1007/s11249-012-9965-0.
[47] M. Fan, D. Yang, X. Wang, W. Liu, H. Fu, DOSS– Based QAILs: as both neat lubricants and lubricant additives with excellent tribological properties and good detergency, Ind. Eng. Chem. Res. 53 (2014) 17952–17960, https://doi.org/10.1021/ie502849w.
[48] X. Fu, L. Sun, X. Zhou, Z. Li, T. Ren, Tribological study of oil-miscible quaternary ammonium phosphites ionic liquids as lubricant additives in PAO, Tribol. Lett. 60 (2015) 23, https://doi.org/10.1007/s11249-015-0596-0.
[49] K.I. Nasser, J.M. Liñeira del Río, E.R. López, J. Fernández, Synergistic effects of hexagonal boron nitride nanoparticles and phosphonium ionic liquids as hybrid lubricant additives, J. Mol. Liq. 311 (2020), https://doi.org/10.1016/j.molliq.2020.113343 113343.
[50] K. Hou, P. Gong, J. Wang, Z. Yang, Z. Wang, S. Yang, Structural and tribological characterization of fluorinated graphene with various fluorine contents prepared by liquid-phase exfoliation, RSC Adv. 4 (2014) 56543–56551, https://doi.org/10.1039/C4RA10313K.
[51] B.T. Seymour, W. Fu, R.A.E. Wright, H. Luo, J. Qu, S. Dai, B. Zhao, Improved lubricating performance by combining oil-soluble hairy silica nanoparticles and an ionic liquid as an additive for a synthetic base oil, ACS Appl. Mater. Interfaces 10 (2018) 15129–15139, https://doi.org/10.1021/acsami.8b01579.
[52] Y. Li, S. Zhang, Q. Ding, H. Li, B. Qin, L. Hu, Understanding the synergistic lubrication effect of 2-mercaptobenzothiazolate based ionic liquids and Mo nanoparticles as hybrid additives, Tribol. Int. 125 (2018) 39–45, https://doi.org/10.1016/j.triboint.2018.04.019.
[53] J. Sanes, M.-D. Avilés, N. Saurín, T. Espinosa, F.-J. Carrión, M.-D. Bermúdez, Synergy between graphene and ionic liquid lubricant additives, Tribol. Int. 116 (2017) 371–382, https://doi.org/10.1016/j.triboint.2017.07.030.
[54] S.A.S. Amiril, E.A. Rahim, S. Syahrullail, A review on ionic liquids as sustainable lubricants in manufacturing and engineering: recent research, performance, and applications, J. Cleaner Prod. 168 (2017) 1571–1589, https://doi.org/10.1016/j.jclepro.2017.03.197.
[55] M.J.G. Guimarey, M.J.P. Comuñas, E.R. López, A. Amigo, J. Fernández, Thermophysical properties of polyalphaolefin oil modified with nanoadditives, J. Chem. Thermodyn. 131 (2019) 192–205, https://doi.org/10.1016/j.jct.2018.10.035.
[56] F. Novotny-Farka, W. Böhme, H. Stabinger, W. Belitsch, The Stabinger Viscometer a new and unique instrument for oil service laboratories, Anton Paar, World Tribology Congress II, Vienna, Austria, 2001.
[57] X. Paredes, O. Fandiño, M.J.P. Comuñas, A.S. Pensado, J. Fernández, Study of the effects of pressure on the viscosity and density of diisodecyl phthalate, J. Chem. Thermodyn. 41 (2009) 1007–1015, https://doi.org/10.1016/j.jct.2009.04.002.
[58] F.M. Gaciño, T. Regueira, L. Lugo, M.J.P. Comuñas, J. Fernández, Influence of Molecular Structure on Densities and Viscosities of Several Ionic Liquids, J. Chem. Eng. Data 56 (2011) 4984–4999, https://doi.org/10.1021/je200883w.
[59] J.M. Liñeira del Río, E.R. López, J. Fernández, F. García, Tribological properties of dispersions based on reduced graphene oxide sheets and trimethylolpropane trioleate or PAO 40 oils, J. Mol. Liq. 274 (2019) 568–576, https://doi.org/10.1016/j.molliq.2018.10.107.
[60] B. Gupta, N. Kumar, K. Panda, S. Dash, A.K. Tyagi, Energy efficient reduced graphene oxide additives: Mechanism of effective lubrication and antiwear properties, Sci. Rep. 6 (2016) 18372, https://doi.org/10.1038/srep18372.
[61] B. Schlüter, R. Mülhaupt, A. Kailer, Synthesis and tribological characterization of stable dispersions of thermally reduced graphite oxide, Tribol. Lett. 53 (2014) 353–363, https://doi.org/10.1007/s11249-013-0275-y.
[62] V. Zin, S. Barison, F. Agresti, L. Colla, C. Pagura, M. Fabrizio, Improved tribological and thermal properties of lubricants by graphene based nano-additives, RSC Adv. 6 (2016) 59477–59486, https://doi.org/10.1039/C6RA12029F.
[63] R. Pamies, M.D. Avilés, J. Arias-Pardilla, T. Espinosa, F.J. Carrión, J. Sanes, M.D. Bermúdez, Antiwear performance of ionic liquid+graphene dispersions with anomalous viscosity-temperature behavior, Tribol. Int. 122 (2018) 200–209, https://doi.org/10.1016/j.triboint.2018.02.020.
[64] Y. Xu, Y. Peng, K.D. Dearn, T. You, J. Geng, X. Hu, Fabrication and tribological characterization of laser textured boron cast iron surfaces, Surf. Coat. Technol. 313 (2017) 391–401, https://doi.org/10.1016/j.surfcoat.2017.02.005.
[65] M. Ratoi, H. Tanaka, B.G. Mellor, J. Sugimura, Hydrocarbon lubricants can control hydrogen embrittlement, Sci. Rep. 10 (2020) 1361, https://doi.org/10.1038/s41598-020-58294-y.
[66] P. Kumar, M.F. Wani, Effect of temperature on the friction and wear properties of graphene nano-platelets as lubricant additive on Al-25Si alloy, Mater. Res. Express 6 (2019), https://doi.org/10.1088/2053-1591/aafb46 046513.

[67] I. Minami, T. Inada, R. Sasaki, H. Nanao, Tribo-chemistry of phosphonium-derived ionic liquids, Tribol. Lett. 40 (2010) 225–235, https://doi.org/10.1007/s11249-010-9626-0.
[68] A. Hernández Battez, M. Bartolomé, D. Blanco, J.L. Viesca, A. Fernández-González, R. González, Phosphonium cation-based ionic liquids as neat lubricants: physicochemical and tribological performance, Tribol. Int. 95 (2016) 118–131, https://doi.org/10.1016/j.triboint.2015.11.015.
[69] A. Hernández Battez, C.M.C.G. Fernandes, R.C. Martins, B.M. Graça, M. Anand, D. Blanco, J.H.O. Seabra, Two phosphonium cation-based ionic liquids used as lubricant additive. Part II: Tribofilm analysis and friction torque loss in cylindrical roller thrust bearings at constant temperature, Tribol. Int. 109 (2017) 496–504, https://doi.org/10.1016/j.triboint.2017.01.020.